Electronic Supplementary Material (ESI) for Journal of Materials Chemistry B.

Supporting Information

Kinetic Stability Modulation of Polymeric Nanoparticles for Enhanced Detection of Influenza Virus via Penetration of Viral Fusion Peptides

Chaewon Park,[a] Jong-Woo Lim,[a] Geunseon Park,[a] Hyun-Ouk Kim,[b] Sojeong Lee,[a] Yuri H. Kwon,[a] Seong-Eun Kim,[c] Minjoo Yeom ,[d] Woonsung Na,[e,f] Daesub Song,[d] Eunjung Kim*[g] and Seungjoo Haam*[a]

[a]Department of Chemical and Biomolecular Engineering, Yonsei University, Seoul 03722, Republic of Korea

[b]Division of Chemical Engineering and Bioengineering College of Art, Kangwon National University, Chuncheon 24341, Republic of Korea

[c]Huvet Bio Inc., Seoul 05836, Republic of Korea

[d]College of Pharmacy, Korea University, Sejong 30019, Republic of Korea

[e]College of Veterinary Medicine, Chonnam National University, Gwangju 61186, Republic of Korea

[f]Animal Medical Institute, Chonnam National University, Gwangju 61186, Republic of Korea

[g]Division of Bioengineering, Incheon National University, Incheon 22012, Republic of Korea

1. Characterization of Leu-NCA

Leucine *N*-carboxyanhydride (Leu-NCA) was synthesized using triphosgene. The chemical structure of Leu-NCA was verified using FT-IR and ^{1}H NMR spectroscopy (**Fig. S1**). In the FT-IR spectra, two prominent characteristic peaks appear at 1800 cm^{-1} and 3331 cm^{-1}, which correspond to the carbonyl (C=O) and secondary amine (-NH-) groups of the anhydride ring of Leu-NCA, respectively. The ^{1}H NMR spectra of the Leu-NCA showed chemical shifts at 6.05 ppm and 1.01 ppm, which can be assigned to protons of secondary amine (-NH-) and protons of methyl groups ($(CH_3)_2$-) in the leucine residues, respectively. As shown in **Fig. S1c**, all proton peaks of *D,L*-leucine and Leu-NCA are identified and assigned in their ^{1}H NMR spectra.

2. Characterization of mPEG-*b*-pLeu

The successful synthesis of methoxypolyethylene glycol-*block*-polyleucine (mPEG-*b*-pLeu) was confirmed by FT-IR analysis (**Fig. S2b and S2e**). The characteristic peaks in the FT-IR spectra are as follows: alkyl C-H stretching and deformation peaks at 2953, 2871, and 1467 cm^{-1}; N-H stretching vibration at 3300 cm^{-1}; amide I vibration at 3060 cm^{-1}; C=O stretching vibration at 1654 cm^{-1}; N-H bending and C-N stretching vibration (amide II) at 1542 cm^{-1}.

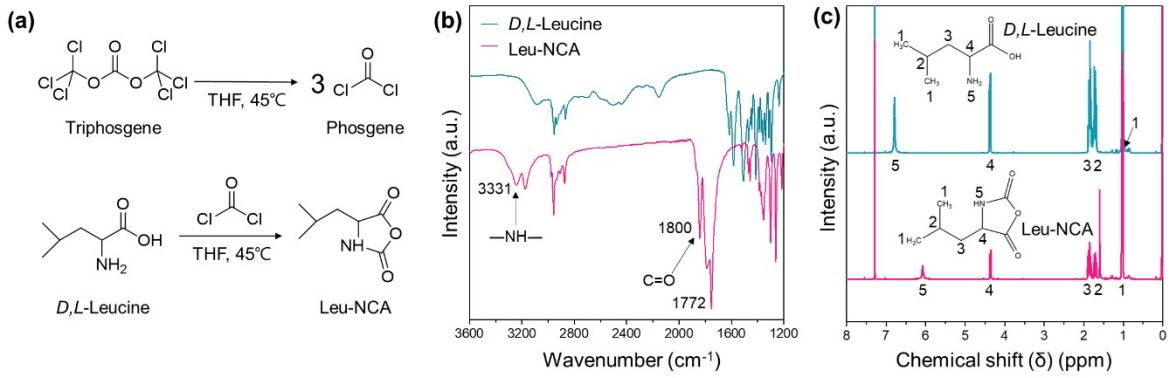

Fig. S1 (a) Schematic of the synthesis of Leu-NCA using triphosgene in anhydrous tetrahydrofuran (THF). (b) FT-IR and (c) ^{1}H NMR spectra of *D,L*-Leucine and Leu-NCA. Chloroform-*d* was used in the NMR measurements.

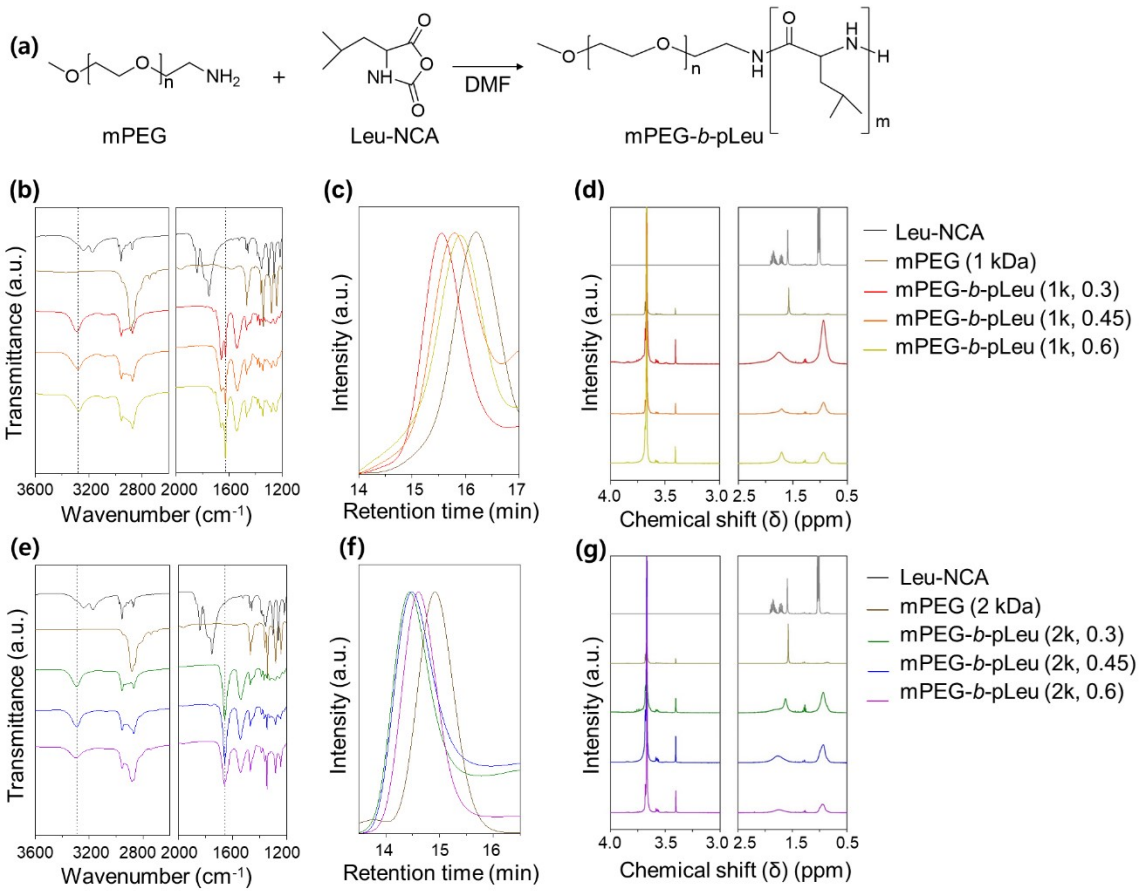

Fig. S2 (a) Schematic of the synthesis of mPEG-*b*-pLeu copolymers using ring-opening polymerization of Leu-NCA. (b–g) Characterization of mPEG-*b*-pLeu copolymers synthesized with 1kDa and 2kDa of mPEG: (b, e) FT-IR spectra, (c, f) GPC traces with anhydrous tetrahydrofuran as mobile phase, and (d, g) ^{1}H NMR spectra in the presence of chloroform-*d*.

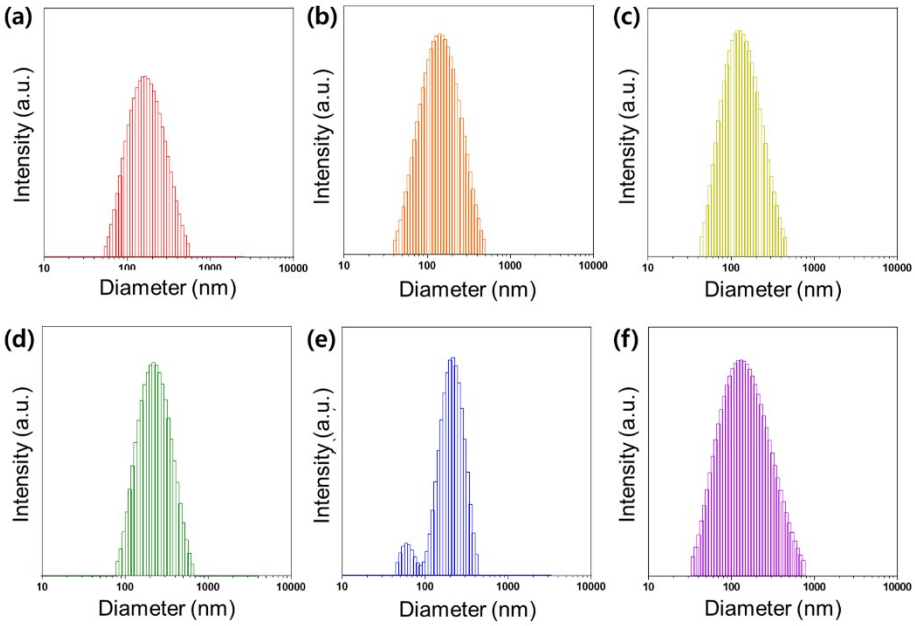

Fig. S3 Hydrodynamic size distributions of PNPs determined by DLS: (a) PNP (1k, 0.3), (b) PNP (1k, 0.45), (c) PNP (1k, 0.6), (d) PNP (2k, 0.3), (e) PNP (2k, 0.45), and (f) PNP (2k, 0.6).

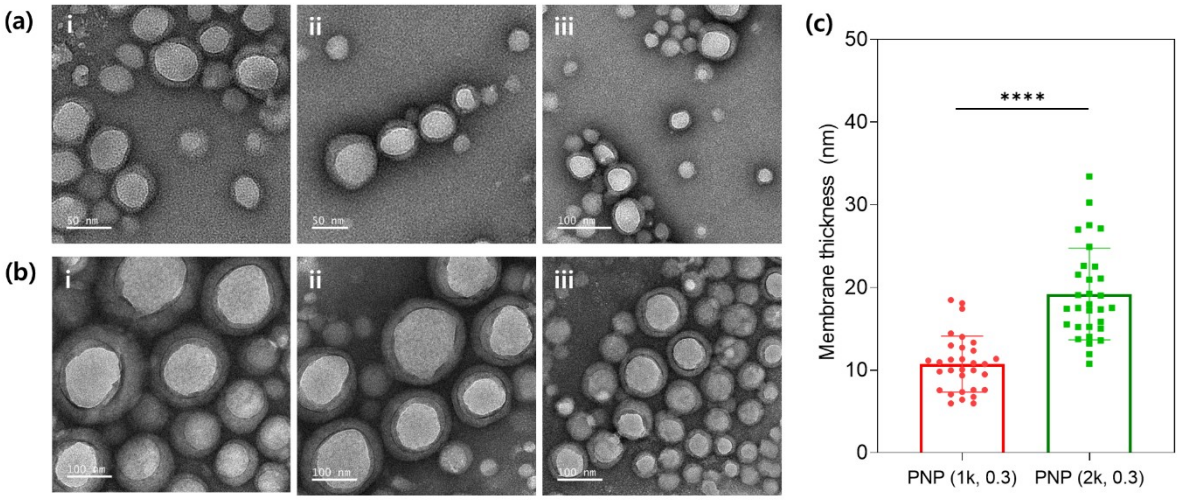

Fig. S4 Representative TEM images of (a) PNP (1k, 0.3) and (b) PNP (2k, 0.3) with negative staining using 3% (w/v) of neutral phosphotungstic acid. (c) Membrane thicknesses of PNP (1k, 0.3) and PNP (2k, 0.3) measured from TEM images. Data represent mean ± standard deviation for the size analysis over 31 particles per PNP. Statistical p-value between two groups is determined using Student's t-test (n = 31, ****$p < 0.0001$).

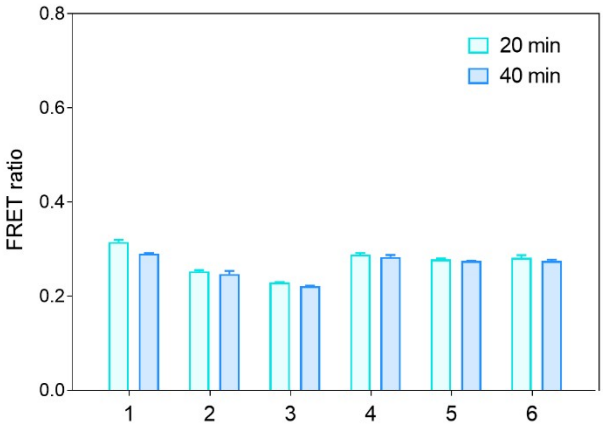

Fig. S5 FRET ratios of the PNPs after 20 and 40 min incubation with 10% (v/v) of Triton X-100 solution. Samples are: 1: PNP (1k, 0.3), 2: PNP (1k, 0.45), 3: PNP (1k, 0.6), 4: PNP (2k, 0.3), 5: PNP (2k, 0.45), and 6: PNP (2k, 0.6). Data represent mean ± standard deviation (n = 3).

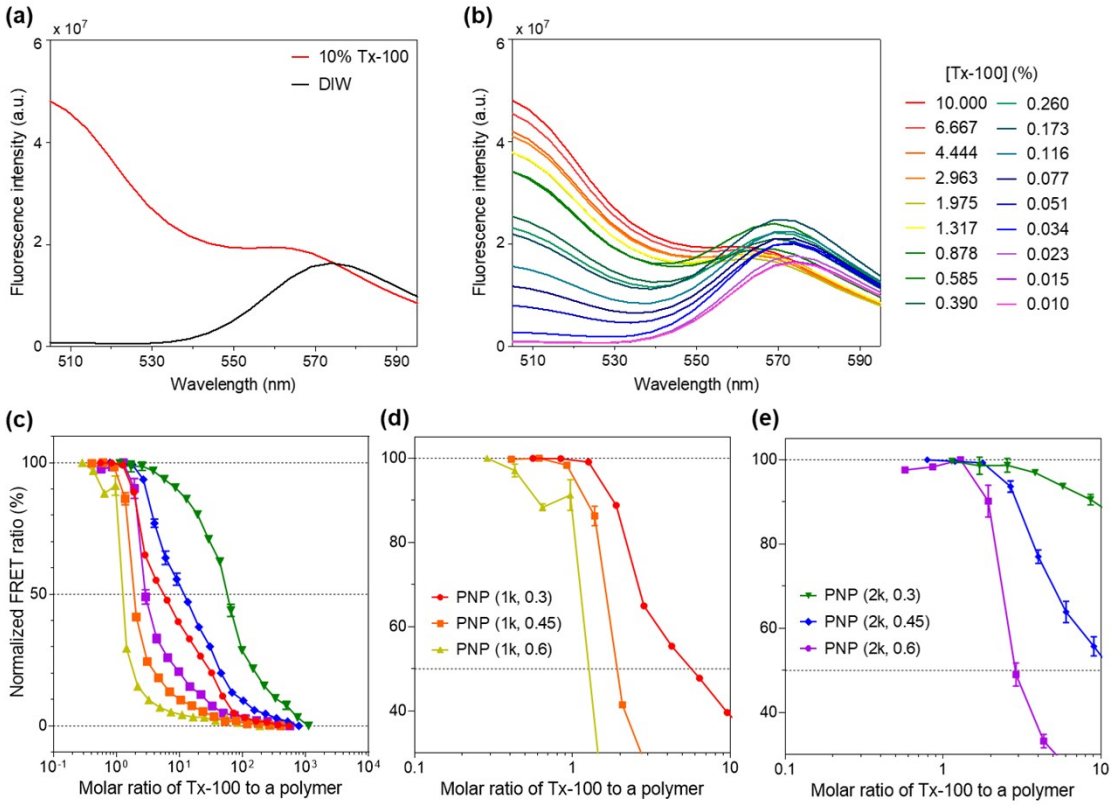

Fig. S6 Solubilization assay. (a) Emission fluorescence spectra of PNP (1k, 0.3) before and after treatment with 10% (v/v) Triton X-100 (Tx-100) (excitation at 475 nm). (b) Representative emission fluorescence spectra of PNP (1k, 0.3) treated with various concentrations of Tx-100 (0.01-10%). (c-e) Normalized FRET ratios of a series of PNPs with increasing amounts of Tx-100 after 40 min: FRET signal profiles of (c) all PNPs, and magnified profiles of (d) PNP (1k) and (e) PNP (2k) in the range of 0.1 to 10 molar ratio of Tx-100 to a polymer. The maximum and minimum FRET ratios were normalized to 100% and 0% FRET ratios, respectively. All fluorescence measurements were carried out after 40 min incubation with Tx-100 at room temperature. Data represent mean ± standard deviation (n = 3).

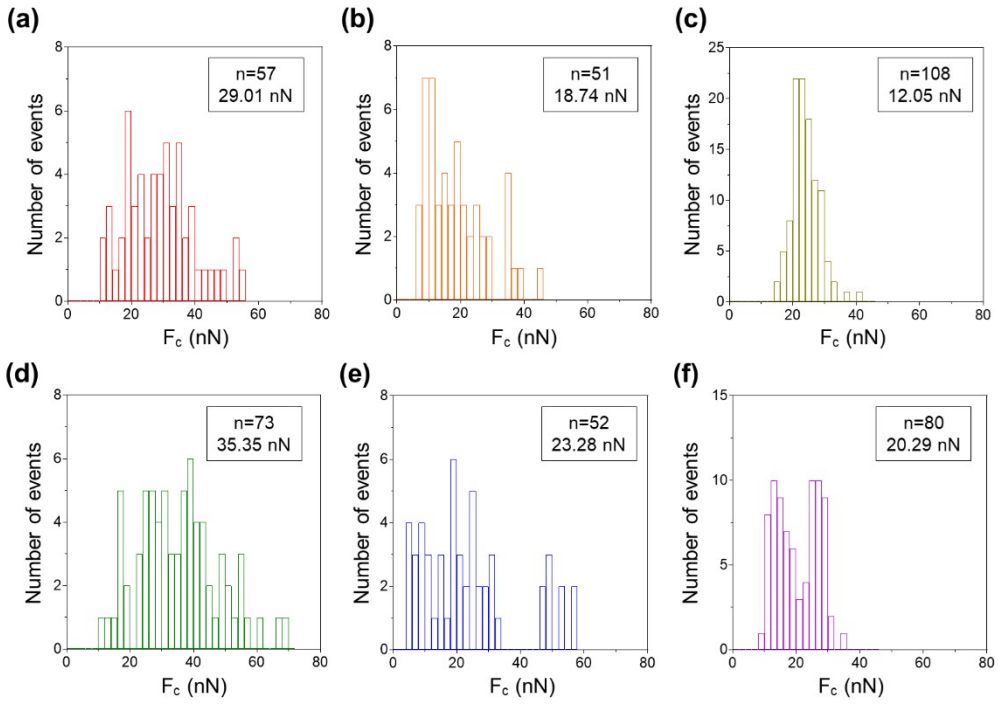

Fig. S7 Histogram of the critical force for initiating PNP rupture (F_c) of (a) PNP (1k, 0.3), (b) PNP (1k, 0.45), (c) PNP (1k, 0.6), (d) PNP (2k, 0.3), (e) PNP (2k, 0.45), and (f) PNP (2k, 0.6) measured by AFM-based nanoindentation tests. The insets represent the number of measurements (*n*) and the estimated average F_c values.

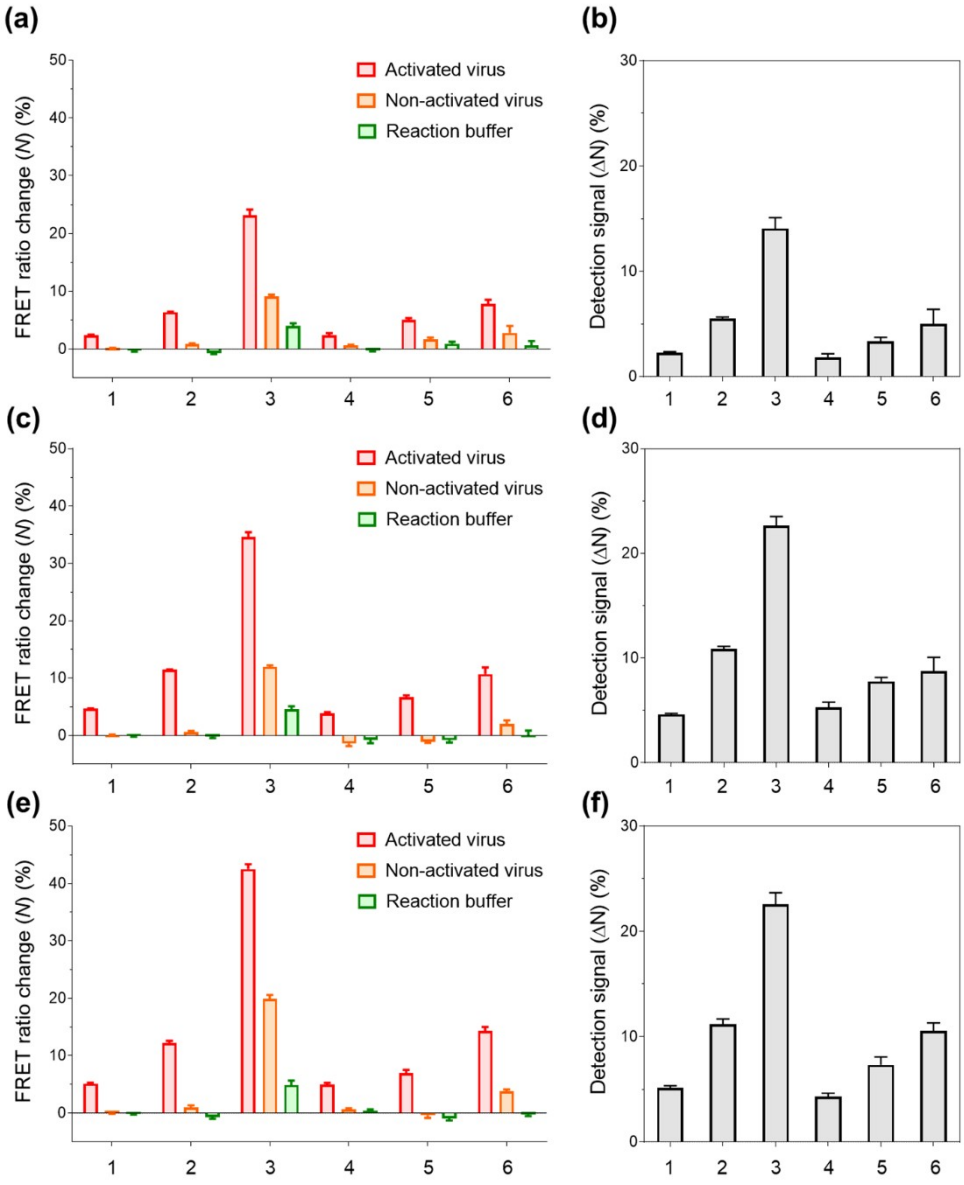

Fig. S8 Influenza virus detection with PNPs. FRET ratio changes (*N*) of PNPs after incubation with (a) CA04(H1N1) ($10^{6.375}$ $TCID_{50}$ mL^{-1}), (c) H4N6 ($10^{4.5}$ $TCID_{50}$ mL^{-1}), and (e) H6N8 ($10^{5.625}$ $TCID_{50}$ mL^{-1}) viruses. Each PNP was incubated with activated viruses in the presence of trypsin and acidic buffer (red), non-activated viruses in the absence of trypsin and acidic buffer (orange), and in a solution containing trypsin and acidic reaction buffer (green). Detection signals obtained from the fusion assay with (b) CA04(H1N1), (d) H4N6, and (f) H6N8 viruses. The average detection signals (*ΔN*) were obtained by subtracting FRET ratio changes of the activated groups from non-activated virus groups. Samples are: 1: PNP (1k, 0.3), 2: PNP (1k, 0.45), 3: PNP (1k, 0.6), 4: PNP (2k, 0.3), 5: PNP (2k, 0.45), and 6: PNP (2k, 0.6). Box plots represent mean ± standard deviation (n = 3).

Table S1. Various nanomaterial-based techniques for the detection of influenza viruses

Nanomaterial	Technique	Analyte	Detection signal	Detection time	Limit of detection	Ref
PNPs	Membrane fusion assay	Influenza A virus (4 subtypes)	Fluorescence	30 min	$10^{2.08}$ $TCID_{50}$/mL	This study
Carbon nanoparticles	Lateral flow immunoassay	Influenza A virus (H1N1 and H3N2)	Colorimetric signal	15-20 min	$10^{2.5}$ $TCID_{50}$/mL	[1]
AuNP coated PS spheres	Lateral flow immunoassay	Influenza A (H3)	Colorimetric signal	5 min	$10^{1.49}$ $TCID_{50}$/mL	[2]
UCNPs	Lateral flow immunoassay	Avian influenza virus	Fluorescence	20 min	10^{2} EID_{50}/mL (H5N2) $10^{3.5}$ EID_{50}/mL (H5N6)	[3]
PGMA-coated PS nanoparticle	Size measurement	Influenza A virus (H1N1 and H3N2)	Diameter distribution	> 1 h	100 pfu/mL or $10^{2.16}$ $TCID_{50}$/mL*	[4]
PANi-encapsulated PNPs	Virus-ligand binding	Influenza A virus (H1N1)	Colorimetric signal	15 min	$10^{3.37}$ $TCID_{50}$/mL	[5]
PDA nanoparticles	Virus-ligand binding	Influenza A virus (H1N1)	Colorimetric signal	5 min	10^{5} pfu	[6]
AuNPs	Virus-ligand binding	Influenza virus (14 subtypes)	Colorimetric signal	90 min	8 HA titer	[7]
AuNPs and CNTs	ELISA	Influenza A virus (H3N2)	Colorimetric signal	> 9 h[a]	10 pfu/mL or $10^{1.15}$ $TCID_{50}$/mL[b]	[8]

[a]The pfu/mL value was divided by a factor of 0.7 to obtain the $TCID_{50}$/mL value for approximate comparison.[9]
[b]Overnight process was assumed as 6 hours or more.
Abbreviations: PNPs, polymeric nanoparticles; AuNP, gold nanoparticles; PS, polystyrene; UCNPs, upconversion nanoparticles; PGMA, poly(methyl methacrylate); PANi, poly(aniline-co-pyrrole); PDA, polydiacetylene; CNTs, carbon nanotubes; ELISA, enzyme-linked immunosorbent assay; HA, hemagglutinin.

References

[1] N. Wiriyachaiporn, H. Sirikett, W. Maneeprakorn, T. Dharakul, *Microchim. Acta* 2017, **184**, 1827-1835.

[2] X. Liu, J. Yang, Q. Li, Y. Wang, Y. Wang, G. Li, J. Shi, P. Ding, J. Guo, R. Deng, G. Zhang, *Microchim. Acta* 2020, **187**, 1-7.

[3] J. Kim, J. H. Kwon, J. Jang, H. Lee, S. Kim, Y. K. Hahn, S. K. Kim, K. H. Lee, S. Lee, H. Pyo, C.-S. Song, J. Lee, *Biosens. Bioelectron.* 2018, **112**, 209-215.

[4] T. Matsubara, A. Kubo, T. Sato, *Polym. J.* 2020, **52**, 261-266.

[5] G. Park, H.-O. Kim, J.-W. Lim, C. Park, M. Yeom, D. Song, S. Haam, *Nano Res.* 2021, 1-9.

[6] S. Song, K. Ha, K. Guk, S. G. Hwang, J. M. Choi, T. Kang, P. Bae, J. Jung, E.-K. Lim, *RSC Adv.* 2016, **6**, 48566-48570.

[7] L. Zheng, J. Wei, X. Lv, Y. Bi, P. Wu, Z. Zhng, P. Wang, R. Liu, J. Jiang, H. Cong, J. Liang, W. Chen, H. Cao, W. Liu, G. F. Gao, Y. Du, X. Jiang, X. Li, *Biosens. Bioelectron.* 2017, **91**, 46–52.

[8] S. R. Ahmed, J. Kim, T. Suzuki, J. Lee, E. Y. Park, *Biosens. Bioelectron.* 2016, **85**, 503-508.

[9] P. J. Jannetto, B. W. Buchan, K. A. Vaughan, J. S. Ledford, D. K. Anderson, D. C. Henley, N. B. Quigley, N. A. Ledeboer, *J. Clin. Microbiol.* 2010, **48**, 3997-4002.